# Design and Implementation of a Fault-Tolerant Magnetic Bearing System for Turbo-Molecular Vacuum Pump

Myounggyu D. Noh, *Member, IEEE*, Seong-Rak Cho, Jin-Ho Kyung, Seung-Kook Ro, and Jong-Kweon Park

***Abstract*—One of the obstacles for a magnetic bearing for use in a wide range of industrial applications is the failure modes associated with magnetic bearings, which are not expected for conventional passive bearings. These failure modes include electric power outage, power amplifier faults, position sensor faults, and the malfunction of controllers. Fault tolerant magnetic bearing systems have been proposed so that the system can operate in spite of some faults in the system. In this paper, we describe the design and implementation of a fault tolerant magnetic bearing system for a turbo-molecular vacuum pump. The system can cope with actuator/amplifier faults, as well as faults in position sensors, which are the two major fault modes in a magnetic bearing system.**

***Index Terms*—Actuators, fault tolerance, magnetic levitation, sensors.**

## Nomenclature

| | |
|---|---|
| $\mathbf{I}$ | Coil current vector. |
| $F_x$ | Force in $x$ direction. |
| $F_y$ | Force in $y$ direction. |
| $\mathbf{W}$ | Current distribution matrix. |
| $C_x$ | Current-to-force constant in $x$ direction. |
| $C_y$ | Current-to-force constant in $y$ direction. |
| $s$ | Sensor output. |
| $\mathbf{A}$ | Sensor sensitivity matrix. |
| $\mathbf{G}_s$ | Sensor gain matrix. |

## I. Introduction

One of the obstacles for a magnetic bearing to be used in a wide range of industrial applications is the failure modes associated with magnetic bearings, which conventional passive bearings do not encounter. These failure modes include electric power outage, power amplifier faults, position sensor faults, and the malfunction of controllers. Fault tolerant magnetic bearing systems have been proposed so that the system can operate in spite of some faults in the system [1]–[3]. For example, a backup battery can supply electricity when an electric power outage occurs. Better yet, rotational kinetic energy of the shaft can be converted into electric energy by reversing the power flow of the electric motor equipped in the system, thereby supplying electricity to the magnetic bearings while the shaft safely touches down to the backup bearings.

Controller faults can be dealt with by using triple modular redundancy (TMR), where three identical controllers are employed to maintain system operation in spite of controller faults [4]. For actuator/amplifier faults, several researchers have proposed algorithms for fault tolerance by utilizing the preexisting redundancy of the actuator [1], [2]. It has been shown through computer simulations that an eight-pole magnetic bearing can sustain a fair amount of load capacity even with three poles failing to produce magnetic forces.

In this paper, we designed a fault tolerant magnetic bearing system for a turbo-molecular vacuum pump. The system can cope with the actuator/amplifier faults, as well as the malfunctioning of position sensors. In order to achieve actuator/amplifier fault tolerance, we used the bias linearization method suggested by Meeker and Maslen [1] in addition to the linear power amplifiers we built in-house. For sensor fault tolerance, we designed a ring-shaped inductive sensor described in [5]. The multipole structure of the ring-shaped sensor made it easy to introduce redundancy in sensing, which we utilized for fault tolerance by a method similar to [6].

We built a prototype turbo-molecular pump and tested the fault tolerance while running the pump up to 4200 r/min. The results shows that the magnetic bearing system can operate even with three simultaneously failing poles out of eight actuator poles, in addition to some partial faults in the position sensor.

## II. System Description

The schematic diagram of the turbo-molecular vacuum pump is shown in Fig. 1. The rotor is driven by a brushless DC motor, and supported by the combination of two radial magnetic bearings and one thrust magnetic bearing. The radial motion of the rotor is detected by two sets of inductive sensors, each providing the radial positions of the rotor in two axes. An eddy-current type position sensor measures the axial motion of the rotor. The first bending mode of the rotor was measured to be around 820 Hz (49 200 r/min). The locations of the bearings and sensors were selected to effectively control the rotor running below the first bending mode. The pump also has two touch-down bearings for startups and shutdowns. Detailed descriptions for the magnetic bearings and sensors are as follows.

Manuscript received March 8, 2004; revised September 16, 2005. Recommended by Guest Editor L. S. Stephens.

M. D. Noh and S.-R. Cho are with the Department of Mechatronics Engineering, Chungnam National University, Daejeon 305-764, Korea (e-mail: mnoh@cnu.ac.kr).

J.-H. Kyung, S.-K. Ro, and J.-K. Park are with the Korea Institute of Machinery and Materials, Daejeon 305-343, Korea (e-mail: jhkyung@kimm.re.kr; cniz@kimm.re.kr; jkpark@kimm.re.kr).

Digital Object Identifier 10.1109/TMECH.2005.859830

1083-4435/$20.00 © 2005 IEEE

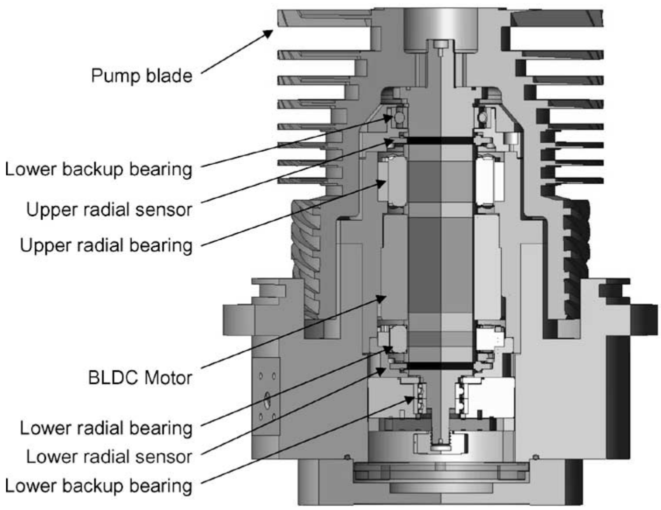


Fig. 1. Schematic diagram of a magnetically levitated turbo-molecular pump.

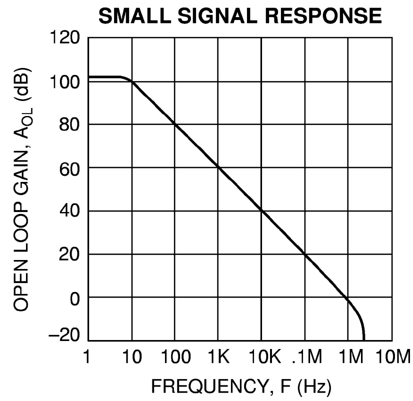


Fig. 2. Open-loop gain of APEX PA21 power op amp [8].

TABLE I
BEARING SPECIFICATIONS

| | Upper Bearing | Lower Bearing |
|---|---|---|
| Air gap (mm) | 0.25 | 0.25 |
| Pole axial length (mm) | 23 | 8.5 |
| Pole width (mm) | 8 | 8 |
| Number of turns per pole | 150 | 150 |
| Inductance per pole (mH) | 21.3 | 7.7 |
| Resistance per pole (Ω) | 1.3 | 0.9 |
| Bias current (A) | 0.3 | 0.3 |
| Actuator gain (N/A) | 113 | 41 |
| Negative stiffness (N/mm) | 154 | 59 |

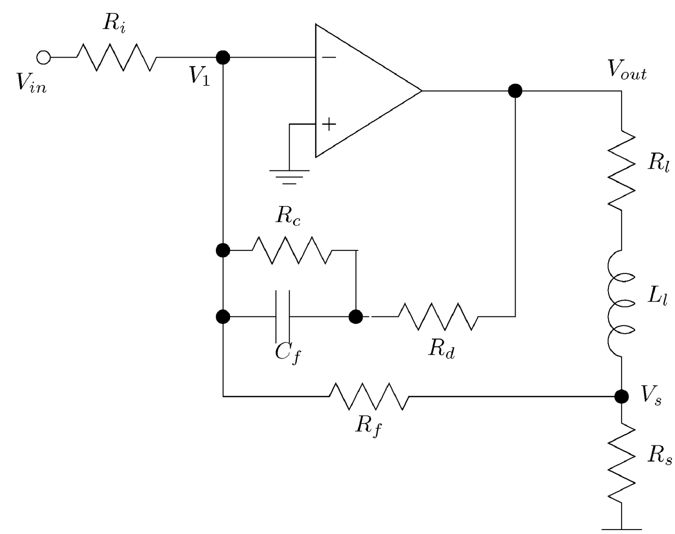


Fig. 3. Schematic of linear transconductance power amplifier.

### A. Radial and Thrust Magnetic Bearings

Each radial bearing has eight poles. For non-fault tolerant operation, two adjacent poles are wired in series (horseshoe configuration). Fault tolerance requires that all eight poles are controlled separately. As illustrated in Fig. 1, the upper bearing is bigger than the lower bearing to counteract the heavy loading due to the pump blade. We chose the lower bearing for the fault tolerance operation. The axial motion of the rotor is controlled by a thrust bearing which consists of two actuator coils and one thrust plate. The specifications of the bearings are summarized on Table I. For startups and shutdowns, the rotor has two backup ball bearings which have the radial clearance of 0.1 mm.

The magnetic bearings are driven by linear transconductance amplifiers. We chose the linear amplifier over a switching type because of the low noise, and the ability to drive resistive loads as well as inductive loads. This is particularly important for fault tolerant operation, because the inductance matrix of the radial bearing becomes singular if all poles are controlled independently [9]. The singularity of the inductance matrix makes the current to force relationship uncontrollable, which means that the coil currents can increase drastically without producing controlled forces on the rotor. In order to avoid this problem, a decoupling choke can be added to the bearing so that the inductance matrix becomes nonsingular. The use of linear amplifiers freed us from designing decoupling chokes which are bulky and require manual tuning.

The linear amplifier is designed around a power operational amplifier. Typical power op amp has a very limited bandwidth. Fig. 2 shows the open-loop gain of the APEX PA21 dual power op amp which we used to implement the amplifier. When used as a transconductance amplifier to drive an inductive load, the limited bandwidth creates a stability problem [7]. The phase margin of the loop gain would be very close to 0 so that the amplifier is susceptible to the noise. The stability of the amplifier can be increased by adding several components in the feedback path. The schematic of the compensated amplifier is shown in Fig. 3. A single pole created by $C_f$ and $R_d$ provides sufficient phase margin. A resistor parallel with $C_f$ decrease the time to reach the steady-state substantially with slight loss in DC gain. The component values of $C_f = 1$ $\mu$F, $R_d = 500$ k$\Omega$, and $R_c = 5$ k$\Omega$ result in a transconductance amplifier with approximately 800 Hz bandwidth and phase margin of 85.8°. The values of the input resistor $R_i$ and feedback resistor are 20 k$\Omega$ and 1 k$\Omega$, respectively. The sensing resistor $R_s$ has the value of 0.1 $\Omega$.

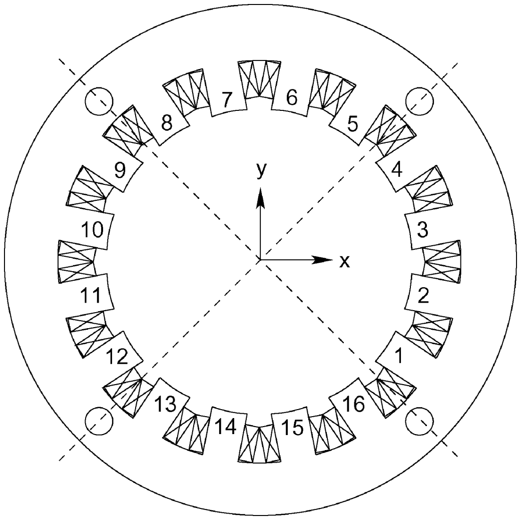


Fig. 4. Schematic of inductive position sensor.

### *B. Position Sensors*

The system is equipped with two sets of inductive sensors for measuring the radial motion of the rotor. Each set of the sensor is a multipolar ring-shaped sensor which produces the radial position of the rotor [5] (see Fig. 4). For non-fault tolerant operation, the 16 poles of the sensor are divided into four groups. Coils of the each group of four poles are wired in series. Two opposing groups differentially sense one axis of the rotor motion. The sensor coils are driven by a PWM switching power amplifier with 50% fixed duty cycle.

The signal processing circuit is composed of the current transducers and the demodulation filter. The demodulation filter is basically a combination of a full-wave rectifier and a low-pass filter. A high-pass filter precedes the demodulation filter to remove any low frequency drift. The block diagram of the signal processing circuit is shown in Fig. 5. The position sensor achieves the resolution of 0.43 $\mu$m with 800-Hz dynamic bandwidth. The nonlinearity error is less than 0.5%.

For fault-tolerant operation, the two adjacent poles of the sensor are wired in series so that one set of the sensor produces four channels. Since number of axes that one sensor needs to measure are two, the signals from these four channels are redundant. The fault-tolerance algorithm takes advantage of this redundancy.

## III. Actuator/Amplifier Fault Tolerance

If a fault occurs in the magnetic bearing or the power amplifier, the consequence of the fault is the same: the loss of coil currents. For fault-tolerant operation, we need to be able to use the functioning coils (or poles) to generate enough levitation force. In this paper, we used the bias linearization method [1]. We will briefly describe the bias linearization algorithm.

In general, a radial magnetic bearing has more poles than the number of the force components that it needs to generate. For example, an eight-pole radial bearing typically generates two force components. Using the magnetic circuit theory, the magnetic force due to the coil currents can be expressed as

$$F_x = \mathbf{I}^T \mathbf{V}_x \mathbf{I} \tag{1}$$

$$F_y = \mathbf{I}^T \mathbf{V}_y \mathbf{I}. \tag{2}$$

In (1) and (2), the current vector $\mathbf{I}$ contains the coil currents, and the matrices $\mathbf{V}_x$ and $\mathbf{V}_y$ are the functions of air gaps, the number of turns per pole, pole face area, etc. With the given coil currents $\mathbf{I}$, the forces $F_x$ and $F_y$ are uniquely determined. However, the inverse relationship of the quadratic (1) and (2) is not unique. Bias linearization provides an optimal solution to this inverse problem [9]. If we choose a current distribution matrix $\mathbf{W}$ such that

$$\mathbf{I} = \mathbf{W} \begin{bmatrix} i_b \\ i_x \\ i_y \end{bmatrix} \tag{3}$$

the force becomes

$$F_x = C_x i_b i_x \tag{4}$$

$$F_y = C_y i_b i_y. \tag{5}$$

For an eight-pole radial magnetic bearing, one example of this current distribution matrix is

$$\mathbf{W} = \begin{bmatrix} 0.5051 & 0.4572 & 0.1894 \\ -0.5051 & -0.1894 & -0.4572 \\ 0.5051 & -0.1894 & 0.4572 \\ -0.5051 & 0.4572 & -0.1894 \\ 0.5051 & -0.4572 & -0.1894 \\ -0.5051 & 0.1894 & 0.4572 \\ 0.5051 & 0.1894 & -0.4572 \\ -0.5051 & -0.4572 & 0.1894 \end{bmatrix}. \tag{6}$$

Fault-tolerance algorithms utilize the bias linearization and the fact there is the redundancy of coil currents. When some of the poles fail, a new current distribution matrix can be used to relate the control currents with the force vector. For example, when the first pole fails, the following current distribution matrix enables the bearing to produce forces without any loss in load capacity

$$\mathbf{W} = \begin{bmatrix} 0 & 0 & 0 \\ -1.01 & -0.6466 & -0.6466 \\ 0 & -0.6466 & 0.2678 \\ -1.01 & 0 & -0.3788 \\ 0 & -0.9145 & -0.3788 \\ -1.01 & -2678 & 0.2678 \\ 0 & -0.2678 & -0.6466 \\ -1.01 & -0.9145 & 0 \end{bmatrix}. \tag{7}$$

Theory tells us that the bearing can produce the force vector in any direction, even with three adjoining poles failing, when the coil selection matrix is

$$\mathbf{W} = \begin{bmatrix} 0 & 0 & 0 \\ 0 & 0 & 0 \\ 0 & 0 & 0 \\ -0.6667 & 0.4483 & -1.5307 \\ 0 & -0.9511 & -2.2961 \\ 0 & -0.9511 & -2.2961 \\ 0 & -0.9511 & -2.2961 \\ -0.6667 & -1.3994 & -0.7654 \end{bmatrix}. \tag{8}$$

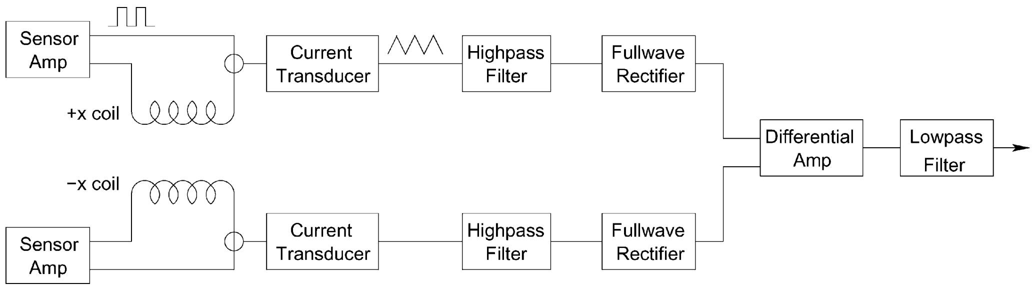


Fig. 5. Block diagram of sensor signal processing circuit.

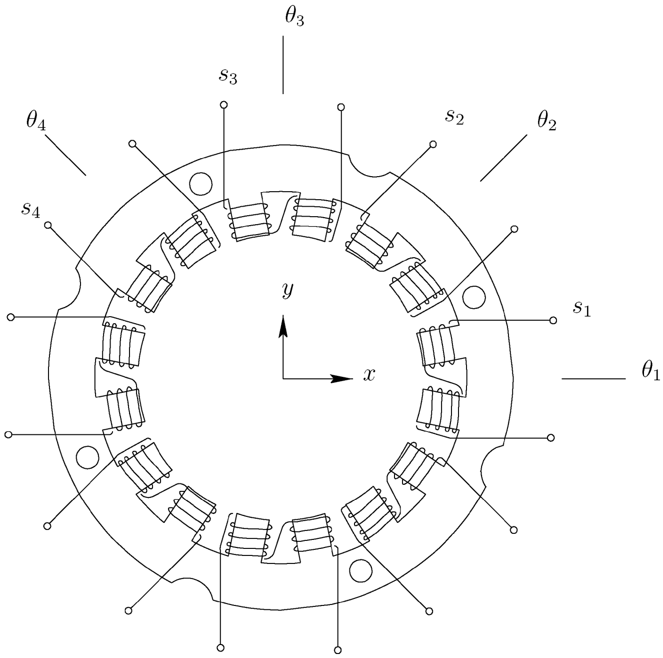


Fig. 6. Fault-tolerant inductive sensor.

In case of three adjoining poles failing, however, the load capacity of the bearing is reduced to 14% of the no-fault case.

## IV. Sensor Fault Tolerance

As in the case of actuator fault-tolerance, a simple way of achieving sensor fault tolerance is by having redundancy. The multipolar structure of the ring-shaped inductive sensor makes it easy to introduce redundancy. As shown in Fig. 6, the coils of two adjacent poles are wired in series for fault-tolerant operation. Two opposing sets of poles forms one sensing channel. Thus, there are four channels $s_1, s_2, s_3$, and $s_4$ in one ring-type inductive sensor. If the angles of each channel are $\theta_1$ through $\theta_4$, the outputs of the four channels are related to the displacement by

$$\begin{bmatrix} s_1 \\ s_2 \\ s_3 \\ s_4 \end{bmatrix} = \begin{bmatrix} \cos\theta_1 & \sin\theta_1 \\ \cos\theta_2 & \sin\theta_2 \\ \cos\theta_3 & \sin\theta_3 \\ \cos\theta_4 & \sin\theta_4 \end{bmatrix} \begin{bmatrix} x \\ y \end{bmatrix}. \tag{9}$$

We can write (9) in a matrix form as

$$\mathbf{s} = \mathbf{A}\mathbf{x}. \tag{10}$$

The inverse of (10) is not unique. We can obtain an optimal solution by using the pseudoinverse

$$\mathbf{x} = (\mathbf{A}^T\mathbf{A})^{-1}\mathbf{A}^T\mathbf{s} = \mathbf{G}_s\mathbf{s}. \tag{11}$$

For example, this optimal solution would be

$$G_s = \begin{bmatrix} 1 & \frac{\sqrt{2}}{2} & 0 & -\frac{\sqrt{2}}{2} \\ 0 & \frac{\sqrt{2}}{2} & 1 & \frac{\sqrt{2}}{2} \end{bmatrix} \tag{12}$$

when all four channels of the sensor are working.

In the case of faults in one channel, we can still obtain the sensor gain matrix $\mathbf{G}_s$ by eliminating the corresponding row in the matrix $\mathbf{A}$ [6]. We will call $\mathbf{G}_{s_i}$ the sensor gain matrix when the $i$-th channel is assumed to be malfunctioning and eliminated. In order to detect the sensor fault, we can compute the position estimates $\mathbf{x}_1$ through $\mathbf{x}_4$ using

$$\mathbf{x}_i = \mathbf{G}_{s_i}\mathbf{s}. \tag{13}$$

For instance, the estimate of the rotor position $\mathbf{x}_1$ would be

$$\mathbf{x}_1 = \begin{bmatrix} 0 & \frac{\sqrt{2}}{2} & 0 & -\frac{\sqrt{2}}{2} \\ 0 & \frac{\sqrt{2}}{4} & \frac{1}{2} & \frac{\sqrt{2}}{4} \end{bmatrix} \begin{bmatrix} s_1 \\ s_2 \\ s_3 \\ s_4 \end{bmatrix} \tag{14}$$

which eliminates $s_1$ from the measurement.

Define the error residual as

$$e_i = \|\mathbf{s} - \mathbf{A}\mathbf{x}_i\|_2. \tag{15}$$

Then, the error residuals should be equal to or very close to zero, if there is no fault. If one of the residuals is large compared to the other three, then the corresponding channel must be faulty. In that case, the position is computed by (13) rather than by (11).

## V. Experimental Setup

Fig. 7 shows the picture of the experimental setup. A DSP controller (dSPACE DS1104) carries out the feedback control for the suspension, and performs the fault-detection and fault tolerance algorithms. The suspension controller is a simple PID (proportional-derivative-integral) type.

For actuator/amplifier fault-detection, Hall-type current sensors (LEM HY-5p) monitor the coil currents. The fault signal is flagged when the error between the current command signal

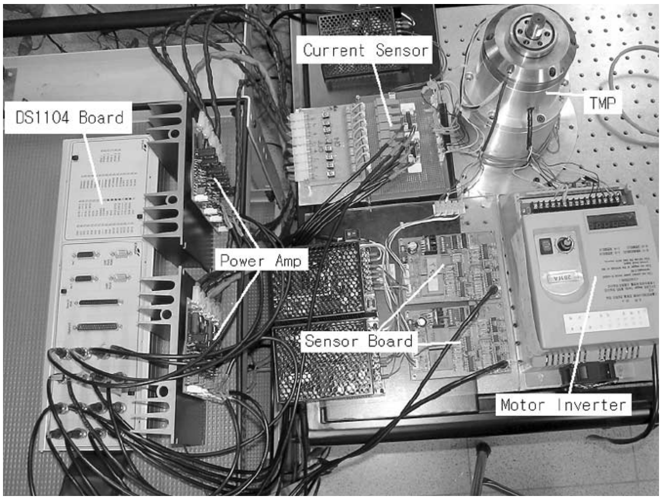


Fig. 7. Experimental setup.

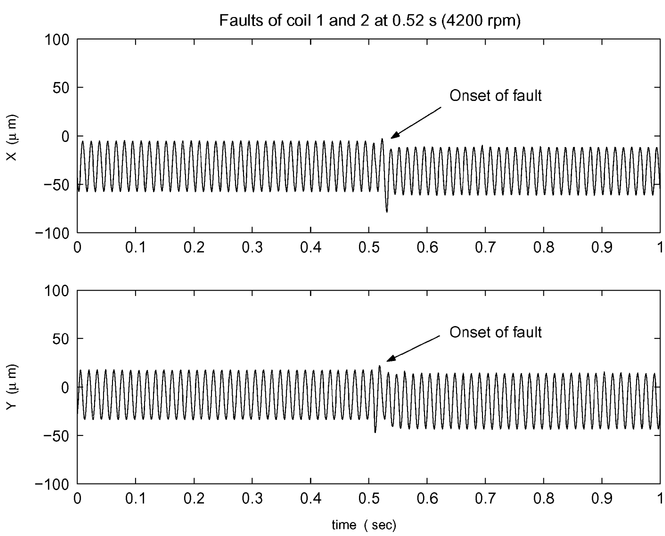


Fig. 8. Rotor positions when coils 1 and 2 are not functioning.

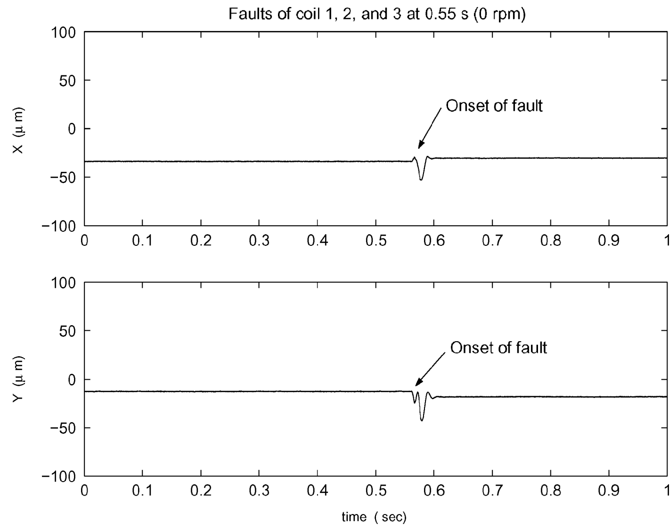


Fig. 9. Rotor positions when coils 1, 2, and 3 are disconnected.

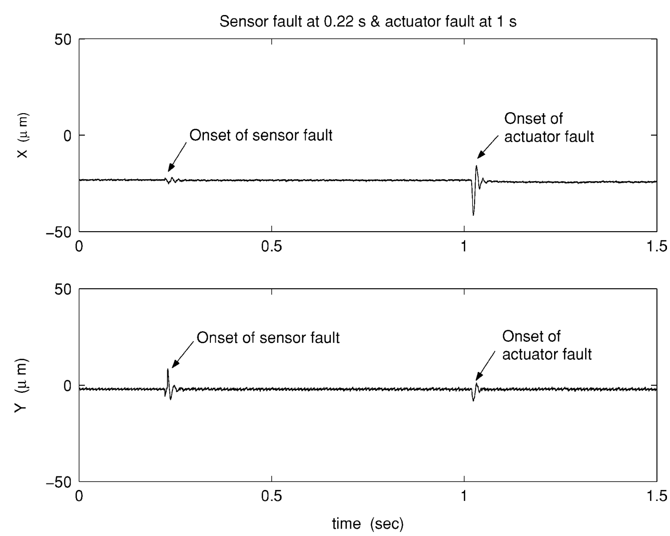


Fig. 10. Rotor positions in the case of simultaneous sensor and actuator faults.

and the actual current is greater than 100 mA for the duration of more than 4 ms, in consideration of the dynamic bandwidth of the current amplifiers and the accuracy of the current sensors. If the controller receives this fault signal, a new current distribution matrix is selected according to the fault condition.

The DSP controller also carries out the fault-detection algorithms for sensor, which is described in Section IV. Basically, the sensor fault-detection algorithm computes the error residuals (see (15)) and sees if any one of them is far off from the rest. If a sensor fault is detected, new position estimates are computed from the remaining signals. Due to the limited number of analog-to-digital and digital-to-analog channels, only the lower radial bearing and lower radial sensor are fault-tolerant. The sampling rate of the controller is 20 kHz.

## VI. Experimental Results and Discussion

Fig. 8 shows the rotor motion when the wires to the two adjacent coils (coil 1 and 2) in the eight-pole radial bearing are manually disconnected from the amplifiers at 0.52 s while the rotor is spinning at 4200 r/min. The proportional gain is 2.4 and the derivative gain is 0.002. The integral gain is set to 0. This result clearly demonstrates the efficacy of the fault-tolerant control. A horseshoe-wired bearing would have gone unstable if one side of the pole-pair had failed.

An extreme case of fault-tolerance is shown in Fig. 9, when three adjacent poles (coils 1, 2, and 3) of the bearing are simultaneously failing. The rotor is at a standstill. Even with three poles failing, the suspension is maintained after a slight adjustment of the center position.

Sensor fault-tolerance is also tested. Fig. 10, shows the rotor positions when the actuator fault occurs while there is a sensor fault. One of four channels in one inductive sensor is disconnected, and coil 1 of the radial bearing is switched off. The results show that the faults does not seem to affect the operation, which demonstrates the adequacy of the fault tolerance algorithms. The rotor is at standstill. The proportional gain is 2.5 and the derivative gain is 0.0065. The integral gain is 1 in this case.

The aforementioned experimental results were obtained from tests that are in no way similar to the actual operating conditions of industrial turbo-molecular pumps. Unfortunately, we were unable to test fault tolerance at the target speed of 40 000 r/min, due to some hardware problems not related to the fault tolerance control described in this paper. However, the fault tolerance control will most likely work at higher pump speeds, as the bandwidths of the actuator and sensors are much higher than the target speed.

The actuator faults described in this paper arise when the bearing coils are open-circuited. The short-circuited faults can be handled in a similar way if the fault tolerance controller utilizes the over-current signal that is usually available in commercial power amplifiers.

## VII. Conclusion

In this paper, we presented our design and implementation a fault tolerant magnetic bearing system for turbo-molecular vacuum pumps. The system can cope with actuator/amplifier faults as well as sensor faults. We took advantage of the preexisting redundancy in the actuator, and used bias linearization for fault tolerance. By independantly controlling the poles of the bearing, we were able to suspend the pump with only five out of eight poles working. We also used the redundancy in the sensor design after reconfiguring the mutipolar ring-shaped inductive sensor. Experimental results demonstrate the adequacy of the fault tolerance algorithms.

## References


[1] E. H. Maslen and D. C. Meeker, “Fault tolerance of magnetic bearings by generalized bias linearization,” *IEEE Trans. Magn.*, vol. 31, no. 3, pp. 2304–2314, May 1995.

[2] U. Na and A. B. Palazzolo, “Fault tolerance of magnetic bearings with material path reluctances and fringing factors,” *IEEE Trans. Magn.*, vol. 36, no. 6, pp. 3939–3946, 2000.

[3] J. P. Lyons, M. A. Preston, R. Gurumoorthy, and P. M. Szczesny, “Design and control of a fault-tolerant active magnetic bearing system for aircraft engine,” in *Proc. 4th Int. Symp. Magnetic Bearings*, ETH Zurich, Zurich, Switzerland, 1994.

[4] E. H. Maslen *et al.*, “Fault tolerant magnetic bearings,” *J. Eng. Gas Turbines Power*, vol. 121, pp. 504–508, Jul. 1999.

[5] M. D. Noh, M. K. Jeong, B. C. Park, J. K. Park, and S. K. Ro, “Development, of low cost inductive sensor using switching noise demodulation,” in *Proc. 8th Int. Symp. Magnetic Bearings*, Mito, Japan, 2002, pp. 311–314.

[6] F. Loesch, “Detection and correction of actuator and sensor faults in active magnetic bearing systems,” in *Proc. 8th Int. Symp. Magnetic Bearings*, Mito, Japan, 2002, pp. 113–118.

[7] Apex Application Note 38, Apex Microtechnology, Tucson, AZ, Loop Stability with Reactive Loads. [Online]. Available: http://www.apexmicrotech.com

[8] PA 21 Data Sheet, Apex Microtechnology, Tucson, AZ. [Online]. Available: http://www.apexmicrotech.com

[9] D. C. Meeker, “Optimal solutions to the inverse problem in quadratic magnetic actuators,” Ph.D. dissertation, Dept. Mech. Aerosp. Eng., Univ. Virginia, Charlottesville, 1995.


**Myounggyu D. Noh** (M’96) received the B.S. the M.S. degrees in mechanical design and production engineering from Seoul National University, Seoul, Korea, in 1986 and 1988, respectively, and the Ph.D. degree in mechanical engineering from the University of Virginia, Charlottesville, in 1996.

From 1996 to 1999, he was a Research Scientist in the Department of Neurosurgery at the University of Iowa, working in the area of functional brain mapping. In 1999, he joined the Faculty of the Department of Mechatronics Engineering at Chungnam National University, Daejeon, Korea, where he currently holds the rank of Associate Professor. From 2004 to 2005, he was a Visiting Scholar at the University of California, Santa Barbara, where, he did consulting work for LaunchPoint Technologies, LLC in the areas of motor and magnetic suspension design for a pediatric ventricular assist device. His research interests include actuator and sensor design, magnetic bearings, and biomedical devices.

**Seong-Rak Cho** received the B.S. degree in mechatronics engineering in 2004 from Chungnam National University, Daejeon, Korea, where he is currently a graduate student in the Department of Mechatronics Engineering.

His research interests are in the fields of electromagnetic actuators, sensorless motor control, and micromagnetic bearing systems.

**Jin-Ho Kyung** received the B.S. degree from Hankook Aviation University, Seoul, Korea, in 1985, and the M.S. and Ph.D. degrees from Korea Advanced Institute of Science and Technology (KAIST), Daejeon, Korea, in 1988, and 2003, respectively.

He is currently a Principal Researcher at the Intelligent Machine Research Center, Korea Institute of Machinery and Materials, Daejeon, Korea. His research interests include active magnetic bearing system design, micromachine tool system analysis, and parallel kinematic machine analysis.

**Seung-Kook Ro** was born in Seoul, Korea, in 1971. He received the B.S. and the M.S. degrees in mechanical engineering from Hankook Aviation University, Seoul, Korea, in 1994 and 1996, respectively. He is currently working toward the Ph.D. degree at Korea Advanced Institute of Science and Technology (KAIST), Daejeon, Korea.

Since 1996, he has been a Senior Researcher at the Intelligent Machine Research Center, Korea Institute of Machinery and Materials, Daejeon, Korea. His research interests are design and control of active magnetic bearing systems, precise actuators using magnetic forces, and machine micro tool systems.

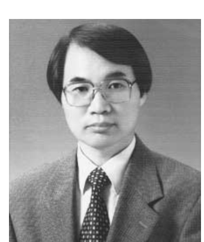

**Jong-Kweon Park** was born in Chungnam, Korea, in 1954. He received the B.S. degree from Inha University, Incheon, Korea, in 1977, and the M.S. and Ph.D. degrees from Changwon National University, Changwon, Korea, in 1990 and 1997, respectively, all in mechanical engineering.

Since 1979, he has been a Principal Researcher at the Intelligent Machine Research Center, Korea Institute of Machinery and Materials, Daejeon, Korea. His research interests are high-speed machine tool system design, and development of micromachine tools and the microfactory.